ISBN: 978-3-95450-214-1 ISSN: 2673-5490 doi:10.18429/JACoW-IPAC2021-MOPAB097

TWO COLOR GRATING DESIGN FOR SOFT X-RAY SELF-SEEDING AT LCLS-II

A. Halavanau, E. Hemsing, D. Morton, G. Marcus
SLAC National Accelerator Laboratory, Stanford University, Menlo Park, CA 94025, USA
G. Wilcox, School of Applied and Engineering Physics,
Cornell University, Ithaca, New York 14853, USA
D. Cocco, Lawrence Berkeley National Laboratory, Berkeley, CA 94720, USA

Abstract

A new grating design is examined for the soft X-ray self-seeding system (SXRSS) at LCLS-II to ultimately produce stable two-color XFEL pulses. The grating performance is analyzed with Fourier optics methods. The final XFEL performance is assessed via full numerical XFEL simulations that substantiate the feasibility of the proposed design.

INTRODUCTION

Soft X-ray self-seeding (SXRSS) system has been successfully designed [1–3] and commissioned at LCLS [4]. It is currently planned for re-commissioning with the new LCLS-II variable-gap undulators. In the present configuration, the SXRSS consists of a grazing incidence toroidal diffraction grating with variable line spacing (VLS), a rotating mirror (M1), a collimation slit, a focusing spherical mirror (M2), and a plane mirror (M3); see Fig. 1. This setup significantly enhances the SXR beam temporal coherence properties and has been a topic of active studies; see e.g., Refs. [5–8].

There is increasing interest in delivering stable two- and multi-color SXR pulses to experiments. At LCLS, multi-color SASE operations were previously achieved by using electron beam-based manipulation techniques, e.g., see Ref [9]. In this paper, we consider an alternative route. We intend to modify the existing SXRSS system with a dual-color grating to produce a self-seeded two-color XFEL pulse. Dual- and multi-color gratings are known in laser optics (e.g., see Refs [10, 11]), but to our knowledge, they have not been applied for self-seeding of XFELs.

Dual- and multi-color self-seeding, combined with the recently proposed enhanced self-seeding approach [12] could lead to a highly stable SXR source, opening new possibilities in time-dependent polarization control [13, 14]. It will also enable new user experiments, e.g., similar to Refs. [15–17].

THEORETICAL MODELLING OF AN IDEAL GRATING

The operational LCLS SXRSS grating parameters were reported in [1–3]. A typical approach for analyzing the idealized grating monochromator properties is through the light path function, which boils down to minimizing the accumulated phase differences over different paths. This model was successfully employed for the initial design and benchmarking of LCLS SXRSS [3]. In this section we review this approach and extend it to the case of an ideal two color grating at LCLS-II.

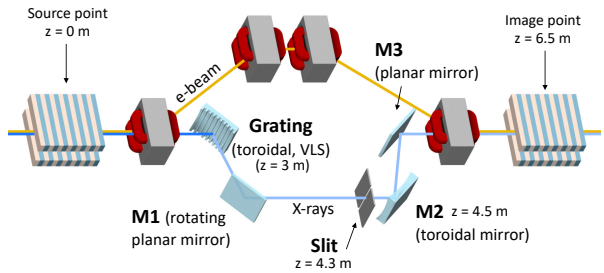

Figure 1: LCLS-II SXR self-seeding system layout (not to scale). The electron beam is propagated through the chicane while photon beam is sent onto the grating. The first diffraction order is apertured at the slit, propagated and refocused onto the electron beam downstream [2].

Fourier Optics Propagation Equations

We start with an initial time-dependent field at a source point A at $z = 0$ m; see Fig. 1. The Fourier transform into the frequency domain is $E_A(\omega, x, y) = \int \bar{E}_A(t, x, y) e^{i\omega t} dt$. The field is propagated through free space from point A to point P on the grating with

$$E_P(\omega, x, y, z_1) = E_A(\omega, x, y) * h(\omega, x, y, z_1), \quad (1)$$

where $*$ is the convolution operator and the classical Fresnel propagator in paraxial approximation is

$$h(\omega, x, y, z) = \frac{k}{2\pi i z} e^{ikz} \exp\left[i \frac{k}{2z} \left[x^2 + y^2 \right] \right]. \quad (2)$$

Here $k = \omega/c$. The effect of the grating is a phase transformation function $T(\omega, x, y)$ on the field modeled as

$$E_g(\omega, x, y, z_1) = E_P(\omega, x, y, z_1) T(\omega, x, y), \quad (3)$$

where $T = \exp\left[i \Delta\Phi_g \right]$. Here $\Delta\Phi_g$ is the additional phase accumulated at the grating. $\Delta\Phi_g$ includes the effects of the grating dispersion, focusing, and higher order aberrations that are not already part of the free-space Fresnel propagation integral, but do appear in the complete diffraction theory of the full light path.

The single color grating has a variable line spacing (VLS) ruling pattern

$$N(x_0) = N_0 + N_1 x_0 + N_2 x_0^2, \quad (4)$$

ISBN: 978-3-95450-214-1 ISSN: 2673-5490 doi:10.18429/JACoW-IPAC2021-MOPAB097

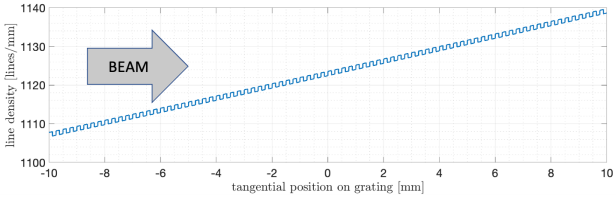

Figure 2: Two color grating density across grating surface assuming a $D = 250$ μm period, $\delta N/N_0 = 0.1\%$, $N_1 = 1.6$ mm^{-2}, and $N_2 = 0.002$ mm^{-3}.

where $N(x_0)$ is the line density of the grooves as a function of transverse coordinate on the grating. The phase tilt due to the N_0 grating ruling is

$$\Delta\Phi_{1,0} = [2\pi N_0 - k(\cos\theta_i - \cos\theta_d)]x_0. \quad (5)$$

The linear density variation N_1 introduces diffraction focusing to minimize deviations in the focus position at the slit across the 250-1300 eV SXRSS tuning range, and the quadratic variation N_2 corrects for spherical aberration.

Since we follow a standard approach to grating theory, we omit further details and refer the reader to the literature [3, 18, 19] for explicit higher-order terms that contribute to the total phase $\Delta\Phi_g = \sum_{i,j}\Delta\Phi_{i,j}$.

In transport simulations through the SXRSS, we account for the unequal incidence and diffraction angles by numerically resizing the wavefront at the grating location by a factor $b = \sin\theta_i/\sin\theta_d$, similarly to [3]. After the grating, the light is propagated through the slit to the focusing mirror location, M2. This is done again with a free-space Fresnel propagator. To include the effect of M2, one can again analyze the light path function and calculate the tangential and sagittal focusing terms $\Delta\Phi_{2,0}, \Delta\Phi_{0,2}$ as well as mirror aberrations, see Ref. [3]. These fields are then used as seed inputs into the XFEL codes GENESIS [20] and GINGER [21] for evaluation of the performance, with both codes showing nearly identical results.

Two-color Flat Grating Equations

The condition $\Delta\Phi_{1,0} = 0$ yields the grating equation for the primary wavevector $k_0 = 2\pi/\lambda_0$,

$$\cos\theta_i - \cos\theta_d = \lambda_0 N_0. \quad (6)$$

Let us now consider a grating that has an alternating pattern of groove densities $N_0^{(1)}, N_0^{(2)}, N_0^{(1)}, N_0^{(2)}\ldots$ in the x_0 direction to produce two colors; see Fig. 2. In this case we can describe the groove density in Eq. (4) as

$$N(x_0) = N_0 + \frac{\delta N}{2} sgn(\sin\kappa x_0) + N_1 x_0 + N_2 x_0^2. \quad (7)$$

This square-wave pattern of switching between $N_0^{(1)}$ and $N_0^{(2)}$ has amplitude $\delta N = N_0^{(2)} - N_0^{(1)}$ and period $D = 2\pi/\kappa$. For $2n\pi < \kappa x_0 < (2n+1)\pi$ the grating density is $N_0 + \frac{\delta N}{2} = N_0^{(2)}$, while for $(2n-1)\pi < \kappa x_0 < 2n\pi$ the grating density is $N_0 - \frac{\delta N}{2} = N_0^{(1)}$. Note that the VLS aspect of the single color grating design is maintained. The two color phase tilt is then

$$\Delta\Phi_{1,0} = [2\pi N_0 - k(\cos\theta_i - \cos\theta_d) + \pi\delta N sgn(\sin\kappa x_0)]x_0. \quad (8)$$

The modified two-color grating equation is then:

$$\cos\theta_i - \cos\theta_d = \frac{2\pi}{k}\left(N_0 \pm \frac{\delta N}{2}\right). \quad (9)$$

Such a grating sends the first diffraction order of two wavevectors into the same diffraction angle. We can define wavenumbers k_1 and k_2 that satisfy the modified grating condition for the groove densities $N_0 - \frac{\delta N}{2} = N_0^{(1)}$ and $N_0 + \frac{\delta N}{2} = N_0^{(2)}$ respectively. At the common diffraction angle the relative line density difference equals the total color separation,

$$\frac{\delta N}{N_0} = \frac{k_2 - k_1}{k_0} = \frac{\delta\omega}{\omega_0}. \quad (10)$$

To seed and amplify two colors, the relative difference in line densities should be less than the relative incoming RMS SASE bandwidth ρ. The typical FEL parameter for SXR operations is $\rho \approx 2\times10^{-3}$, which yields a FEL bandwidth of about 1 eV for the operational photon wavelength range. At this close separation, the VLS terms of the single color grating are sufficient to preserve baseline focusing and aberration correction for both colors.

It is important to note that the ruling of the individual stripes $N_0^{(1)}$ and $N_0^{(2)}$ should be phase-locked across the grating to maintain good seeding into both colors, including the VLS. Further, the periodic stripe ruling also produces frequency sidebands in the diffracted output. These sidebands can lie within the seeded FEL bandwidth to produce additional colors if $1/DN_0 < 2\rho$. To preserve the pure two color mode, this compels making D small enough to push the sidebands outside the FEL bandwidth, or to dither the stripe widths to wash out sidebands. Either way, this must be balanced with the practical aspect of minimizing the impact of the transition region due to manufacturing between stripes if D is made too small. Assuming a transition region of about 10 μm, this gives a range of about $D = 100 - 400$ μm with a target of $D = 250$ μm for the SXRSS parameters.

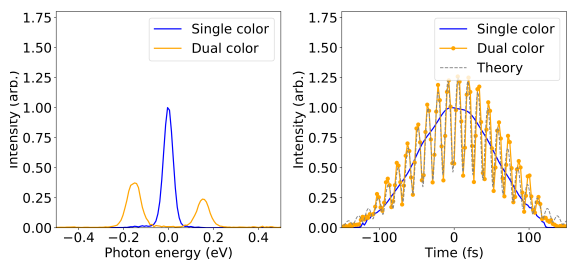

Figure 3: Single- and dual-color seed intensity comparison with $\sigma_\omega = 25.5$ meV grating bandwidth (at 310 eV) in the spectral (left) and temporal (right) domains. The dual-color field was produced from an average of SASE pulses generated upstream of the grating.

ISBN: 978-3-95450-214-1 ISSN: 2673-5490 doi:10.18429/JACoW-IPAC2021-MOPAB097

The two seed colors interfere in the time domain to produce an intensity modulation with period $2\pi/\delta\omega = 2\pi N_0/\omega_0\delta N$, which ranges from about 14 fs at 300 eV to 3.5 fs at 1200 eV for $\delta N/N_0 = 0.1\%$. We note that the relative phase difference between the two colors may fluctuate shot-to-shot due to the random phases of incoming the SASE spikes. Operating with the enhanced self-seeding technique, the relative phase jitter will be drastically suppressed [12].

TWO-COLOR GRATING EXAMPLE CALCULATION AND XFEL SIMULATIONS

We now investigate some practical aspects of our proposed two-color system via numerical simulations. We set the square-wave period to $D = 250$ μm and δN=1.123 lines/mm. The rest of the grating and optical transport parameters are chosen to be identical to the single color design [1–3]. An example simulation using 310 eV photons (λ_0 =4 nm) averaged over multiple GENESIS SASE shots is shown in Fig. 3. As predicted by Eq. (10), the separation between the two colors is 0.31 eV at 310 eV with a $\delta N/N_0 = 0.1\%$ line density variation.

In the XFEL seed amplifier simulations we considered LCLS-II beam with 1.5 kA, 0.4 MeV RMS energy spread and 0.4 μm emittance. The results of an example simulation with GINGER on an ideal 65 fs tophat beam profile are presented in Fig. 4. The temporal fringe spacing from Fig. 3 was used for seeding at the 50 kW level. In the initial stages of amplification, the FEL behaves as a linear amplifier, mimicking the seed pulse shape; see Fig. 4 (top). As the FEL process starts to saturate (Fig. 4, middle), nonlinear growth reduces the fringe contrast, while radiation slippage effects shorten the temporal spike duration. Finally, in the post-saturation regime (Fig. 4, top), the pronounced spikes become about 1 fs FWHM in duration. Depending on the required application, we note that the number of temporal spikes can be adjusted in principle by manipulating the electron beam length, as afforded by the seed pulse duration. In addition, increasing the photon energy will result in larger absolute two-color separation, and per $2\pi N_0/\omega_0\delta N$, will reduce the temporal spike durations. We further point out that the residual SASE pedestal between the temporal spikes in the post-saturation regime may be further reduced with tapering and the use of phase-shifters. This is an ongoing study and the results will be reported elsewhere.

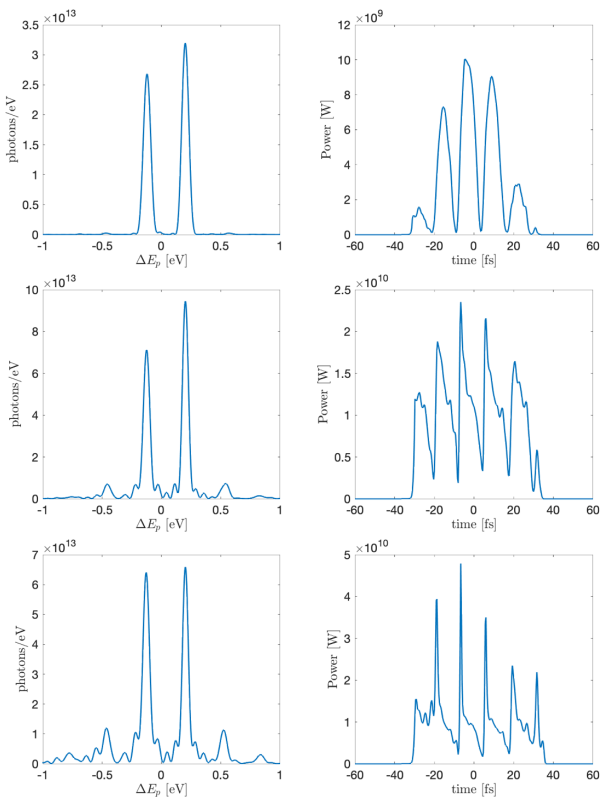

Figure 4: GINGER simulation of two-color seeding at 310 eV (4 nm) with 0.31 eV separation in the exponential (top), pre-saturation (middle) and post-saturation (bottom) regimes. Temporal pulse front is to the left.

SUMMARY

We have presented a design for two-color SXR grating, containing an alternating pattern of grove densities. We explored theoretically and numerically the grating properties, as well as the final seeded XFEL performance. We note that our scheme is not limited to two frequencies and can be extended to multiple-color seeding.

ACKNOWLEDGEMENTS

This work is supported by the U.S. Department of Energy Contract No. DE-AC02-76SF00515 and award no. 2017-SLAC-100382.

REFERENCES

[1] D. Cocco *et al.*, "The optical design of the soft x-ray self-seeding at LCLS", in *Proc. Vol. 8849, X-Ray Lasers and Coherent X-Ray Sources: Development and Applications X:88490A*, Sep. 2013, pp. 31–38. doi:10.1117/12.2024402

[2] Y. Feng, J. Amann, D. Cocco, C. Field, *et al.*, "System design for self-seeding the LCLS at soft x-ray energies", in *Proc. FEL'12*, Nara, Japan, Aug. 2012, paper TUOBI01, pp. 205–212.

[3] S. Serkez, J. Krzywinski, Y. Ding, and Z. Huang, "Soft x-ray self-seeding simulation methods and their application for the linac coherent light source", *Phys. Rev. ST Accel. Beams*, vol. 18, p. 030 708, Mar. 2015. doi:10.1103/PhysRevSTAB.18.030708

[4] D. Ratner *et al.*, "Experimental demonstration of a soft x-ray self-seeded free-electron laser", *Phys. Rev. Lett.*, vol. 114, p. 054 801, Feb. 2015. doi:10.1103/PhysRevLett.114.054801

[5] G. Marcus *et al.*, "Experimental observations of seed growth and accompanying pedestal contamination in a self-seeded, soft x-ray free-electron laser", *Phys. Rev. Accel. Beams*, vol. 22, p. 080 702, Aug. 2019. doi:10.1103/PhysRevAccelBeams.22.080702

ISBN: 978-3-95450-214-1 ISSN: 2673-5490 doi:10.18429/JACoW-IPAC2021-MOPAB097

[6] E. Hemsing, A. Halavanau, and Z. Zhang, "Statistical theory of a self-seeded free electron laser with noise pedestal growth", *Phys. Rev. Accel. Beams*, vol. 23, p. 010 701, Jan. 2020. doi:10.1103/PhysRevAccelBeams.23.010701

[7] Z. Zhang, G. Marcus, E. Hemsing, W. M. Fawley, Z. Huang, and A. Lutman, "Statistical analysis of a self-seeded x-ray free-electron laser in the presence of the microbunching instability", *Phys. Rev. Accel. Beams*, vol. 23, p. 010 704, Jan. 2020. doi:10.1103/PhysRevAccelBeams.23.010704

[8] E. Hemsing *et al.*, "Soft x-ray seeding studies for the slac linac coherent light source ii", *Phys. Rev. Accel. Beams*, vol. 22, p. 110 701, Nov. 2019. doi:10.1103/PhysRevAccelBeams.22.110701

[9] A. A. Lutman *et al.*, "Fresh-slice multicolour x-ray free-electron lasers", *Nature Photonics*, vol. 10, no. 11, pp. 745–750, Nov. 2016. doi:10.1038/nphoton.2016.201

[10] B. Hajj, L. Oudjedi, J.-B. Fiche, M. Dahan, and M. Nollmann, "Highly efficient multicolor multifocus microscopy by optimal design of diffraction binary gratings", *Scientific Reports*, vol. 7, no. 1, p. 5284, Jul. 2017. doi:10.1038/s41598-017-05531-6

[11] D. C. Skigin and R. A. Depine, "Diffraction by dual-period gratings", *Appl. Opt.*, vol. 46, no. 9, pp. 1385–1391, Mar. 2007. doi:10.1364/AO.46.001385

[12] E. Hemsing, A. Halavanau, and Z. Zhang, "Enhanced self-seeding with ultrashort electron beams", *Phys. Rev. Lett.*, vol. 125, p. 044 801, Jul. 2020. doi:10.1103/PhysRevLett.125.044801

[13] N. Sudar, R. Coffee, and E. Hemsing, "Coherent x rays with tunable time-dependent polarization", *Phys. Rev. Accel. Beams*, vol. 23, p. 120 701, Dec. 2020. doi:10.1103/PhysRevAccelBeams.23.120701

[14] J. Morgan and B. W. J. McNeil, "Attosecond polarization modulation of x-ray radiation in a free-electron laser", *Phys. Rev. Accel. Beams*, vol. 24, p. 010 701, Jan. 2021. doi:10.1103/PhysRevAccelBeams.24.010701

[15] G. Geloni and V. Kocharyan and T. Mazza and M. Meyer and E. Saldin and S. Serkez, "Opportunities for Two-color Experiments at the SASE3 undulator line of the European XFEL", 2017. arXiv:1706.00423.

[16] N. Berrah *et al.*, "Femtosecond-resolved observation of the fragmentation of buckminsterfullerene following x-ray multiphoton ionization", *Nature Physics*, vol. 15, no. 12, pp. 1279–1283, Dec. 2019. doi:10.1038/s41567-019-0665-7

[17] S. Schreck *et al.*, "Atom-specific activation in co oxidation", *The Journal of Chemical Physics*, vol. 149, no. 23, p. 234 707, 2018. doi:10.1063/1.5044579

[18] M. Itou, T. Harada, and T. Kita, "Soft x-ray monochromator with a varied-space plane grating for synchrotron radiation: Design and evaluation", *Appl. Opt.*, vol. 28, no. 1, pp. 146–153, Jan. 1989. doi:10.1364/AO.28.000146

[19] M. Fujisawa *et al.*, "Varied line-spacing plane grating monochromator for undulator beamline", *Review of Scientific Instruments*, vol. 67, no. 2, pp. 345–349, 1996. doi:10.1063/1.1146621

[20] S. Reiche, "GENESIS 1.3: a fully 3D time-dependent FEL simulation code", *Nuclear Instruments and Methods in Physics Research A*, vol. 429, pp. 243–248, Jun. 1999. doi:10.1016/S0168-9002(99)00114-X

[21] W. M. Fawley, "A user manual for ginger and its post-processor xplotgin", Berkley, CA, USA, Rep. LBNL-4925, Feb. 2002.